Network modules and hubs in plant-root fungal biomes

Authors: Hirokazu Toju,[1] Satoshi Yamamoto,[2] Akifumi S. Tanabe,[3] Takashi Hayakawa,[4, 5] Hiroshi S. Ishii[6]

Affiliations:

[1]Graduate School of Human and Environmental Studies, Kyoto University, Sakyo, Kyoto 606-8501, Japan.

[2]Graduate School of Human Development and Environment, Kobe University, 3-11, Tsurukabuto, Nada-ku, Kobe 657-8501, Japan.

[3]National Research Institute of Fisheries Science, Fisheries Research Agency, 2-12-4 Fukuura, Kanazawa- ku, Yokohama, Kanagawa 236–8648, Japan.

[4]Department of Wildlife Science (Nagoya Railroad Co., Ltd.), Primate Research Institute, Kyoto University, Inuyama, Aichi 484-8506, Japan.

[5]Japan Monkey Centre, Inuyama, Aichi 484-0081, Japan.

[6]Department of Environmental Biology and Chemistry, Graduate School of Science and Engineering, University of Toyama, 3190 Gofuku, Toyama 930-8555, Japan.

Short title:

Networks of symbionts in plant roots

Subject Areas:

ecology, evolution, network science

Keywords:

alternative stable states, community ecology, enterotypes, Illumina MiSeq, mutualism, network theory

Author for correspondence:

e-mail: toju.hirokazu.4c@kyoto-u.ac.jp

Tel, +81-75-753-6766; Fax +81-75-753-2957.

Abstract

Terrestrial plants host phylogenetically and functionally diverse groups of belowground microbes, whose community structure controls plant growth/survival in both natural and agricultural ecosystems. Therefore, understanding the processes by which whole root-associated microbiomes are organized is one of the major challenges in ecology and plant science. We here report that diverse root-associated fungi can form highly compartmentalized networks of coexistence within host roots and that the structure of the fungal symbiont communities can be partitioned into semi-discrete types even within a single host plant population. Illumina sequencing of root-associated fungi in a monodominant south beech forest revealed that the network representing symbiont–symbiont co-occurrence patterns was compartmentalized into clear modules, which consisted of diverse functional groups of mycorrhizal and endophytic fungi. Consequently, terminal roots of the plant were colonized by either of the two largest fungal species sets (represented by *Oidiodendron* or *Cenococcum*). Thus, species-rich root microbiomes can have alternative community structures as recently shown in the relationships between human gut microbiome type (i.e., "enterotype") and host individual health. This study also shows an analytical framework for pinpointing network hubs in symbiont–symbiont networks, leading to the working hypothesis that a small number of microbial species organize the overall root-microbiome dynamics.

1. Introduction

Since their colonization to terrestrial biosphere 470 million years ago, land plants have coevolved with diverse mutualistic and pathogenic microbes in soil [1-4]. Mycorrhizal fungi and various lineages of rhizosphere bacteria, for instance, enhance plant nutritional states and/or protect hosts from pathogenic soil microbes [2, 5, 6]. As plant growth and health is highly dependent on those root-associated microbes, understanding factors determining the structure of plant-root microbiomes is one of the major challenges in ecology and plant science [2, 5]. However, the diversity of belowground fungi and bacteria is enormous [7-9], making it difficult to reveal the key ecological processes that control the entire community structure of root-associated microbes.

Although uncovering the determinants of microbiome structure is difficult not only in plant–belowground-microbe interactions but also in other host–symbiont systems, recent findings in human-gut microbe studies have revolutionized our views on the formation of microbiomes within/on host organisms [10-12]. Those studies have shown that human individuals are grouped into some major clusters defined by gut bacterial community structure and that such “enterotypes” may be organized by facilitative and competitive interactions among microbial symbionts within hosts [10, 13, 14]. Moreover, an increasing number of studies have revealed close relationships between enterotypes and human health [12], illuminating the importance of symbiont–symbiont interactions in the performance of host individuals [11]. These analytical and conceptual frameworks developed in human enterotype studies are expected to make substantial contributions to plant science. Nonetheless, the existence of classifiable “rhizotypes” [5] of plant-root microbiomes remains to be explored despite its potential importance in the diagnostics and control of root-associated microbial communities.

Here we show a network depicting symbiont–symbiont co-occurrence patterns in hosts and examine whether discrete sets of symbiont community structures actually exist even within a single population of a single plant species. Among the major groups of belowground plant–fungus interactions, we focus on ectomycorrhizal symbiosis [2]. Ectomycorrhizal fungi on the same host plant species potentially compete with each other for space and resources, and several pairs of them are known to show segregated (mutually exclusive) distribution patterns across host individuals as expected by competitive exclusion processes [15-17]. On the contrary, pairs of fungi in facilitative interactions, especially those showing functional complementarity, may coexist within the same terminal root tissue, displaying more aggregated patterns than expected by chance [18]. In addition, fungi adapting to the same soil or host physiological environments are expected to show correlated distribution patterns [19]. Therefore, we predicted that such segregated and aggregated patterns were indicative of potential symbiont–symbiont direct interactions and/or correlated environmental adaptation within host root systems and conducted high-throughput DNA barcoding analysis [4, 20] to reveal how the network of symbiont–symbiont co-occurrence patterns [10, 13] was structured throughout a plant population. Furthermore, to uncover how multiple phylogenetic and functional groups of fungi constitute the entire network, we also took into account fungi belonging to non-ectomycorrhizal lineages. Endophytic fungi, in particular, are conspicuous

in their prevalent infection to plants, but their roles in belowground microbiomes have been poorly understood [4, 21, 22]. By targeting all phylogenetic lineages in the kingdom Fungi, we revealed how the entire symbiont–symbiont network could be structured in a single plant population.

2. Materials and methods

2.1 Sampling

Sampling was conducted in a temperate forest of *Fuscospora cliffortioides* (Hook.f.) Heenan & Smissen (Nothofagaceae) [23] in the Queenstown Lakes District, New Zealand (44º26′00′′S, 169º15′40′′E) from January 16 to 20, 2014. As the *Fuscospora* species was the only tree species that reached the canopy of the forest, it provided an ideal research system for inferring how symbiont–symbiont interactions were structured in a wild host plant population. Along a 687-m mountain trail, we collected 2-cm segments of terminal root samples at 3-cm below the soil surface at 1-m horizontal intervals. The altitudes of the sampling points varied from 862 m (sample no. 1) to 710 m (sample no. 688). The collected 688 samples were carefully washed to remove adhering soil and immediately dried with ample silica gel.

As DNA-barcoding-based analysis *per se* does not provide any information of the nature of symbioses between plants and their root-associated fungi, we use the word “symbionts” to refer to observed fungi irrespective of their potential effects to host plants (i.e., “symbiosis” in broad sense; [24]). Although taxonomic information may help to infer potential ecological roles of each fungus, it is important to acknowledge that fungi detected through high-throughput sequencing can be not only mutualistic, but also commensalistic or antagonistic to their host plants [4].

2.2 Molecular analysis

Each of the 688 samples was pulverized with 4-mm zirconium balls using TissueLyser II (Qiagen) [22] and host plant and fungal symbiont DNA was simultaneously extracted with the cetyltrimethylammonium bromide method [25]. For the molecular identification of fungal symbionts, the nuclear internal transcribed spacer 1 (ITS1) region of fungi was

PCR-amplified. In the PCR amplification of fungal ITS region, we used the forward primer ITS5 [26] fused with 6-mer Ns (for improved "chastity" in Illumina sequencing) [27] and the forward Illumina sequencing primer (5'- TCG TCG GCA GCG TCA GAT GTG TAT AAG AGA CAG [sequencing primer] - NNNNNN [6-mer Ns] - GGA AGT AAA AGT CGT AAC AAG G [ITS5] -3') and the reverse primer ITS2_KYO2 [28] fused with 6-mer Ns and reverse sequencing primer (5'- GTC TCG TGG GCT CGG AGA TGT GTA TAA GAG ACA G [sequencing primer] - NNNNNN [6-mer Ns] - TTY RCT RCG TTC TTC ATC [ITS2_KYO2] -3'). The PCR reaction was conducted using the buffer and DNA polymerase system of KOD FX Neo (TOYOBO), which has proof-reading ability, with a temperature profile of 94ºC for 2 min, followed by 35 cycles at 98ºC for 10 s, 50ºC for 30 s, 68ºC for 50 s, and a final extension at 68ºC for 5 min. Illumina sequencing adaptors were added in the subsequent PCR process using a forward fusion primer consisting of P5 Illumina adaptor, 8-mer index tags for sample identification [29] and 5'-end of the sequencing adaptor (5'- AAT GAT ACG GCG ACC ACC GAG ATC TAC AC [P5 adaptor] - XXXXXXXX [8-mer tag] - TCG TCG GCA GCG TC [sequencing primer] -3') and a reverse fusion primer (5'- CAA GCA GAA GAC GGC ATA CGA GAT [P7 adaptor] - XXXXXXXX [8-mer tag] - GTC TCG TGG GCT CGG [sequencing primer] -3'). The additional PCR reaction was conducted using the KOD FX Neo system with a temperature profile of 94ºC for 2 min, followed by 8 cycles at 98ºC for 10 s, 50ºC for 30 s, 68ºC for 50 s, and a final extension at 68ºC for 5 min.

We also PCR-amplified plant chloroplast *rbcL* and *trnH-psbA* regions to confirm that the sampled roots were those of *F. cliffortioides*. In the first PCR step for the amplification of the two chloroplast regions, we performed a multiplex PCR reaction by mixing equal concentrations of *rbcL* (rbcL_F3 [30] and rbcL_R4 [30]) and *trnH-psbA* (psbA3'f [31] and *trnH* [32]) primers. The multiplex PCR products were then subjected to the second PCR step for adding the index and Illumina adaptor regions. For each step, the buffer/polymerase system and thermal-cycle protocols detailed above were applied.

The indexed PCR products of the 688 samples were pooled into a single library after purification with AMPure XP Kit (Beckman Coulter). The ratio of sample volume to AMpure volume was set to 1:0.6 [27] to remove remaining PCR primers. In the library, the ratio of ITS1 products to *rbcL*/*trnH-psbA* products was set to 4:1. The pooled library was then

subjected to an Illumina Miseq run (run center: Graduate School of Human and Environmental Studies, Kyoto University [KYOTO-HE]) with the 2 × 300 cycle sequencing kit (20% PhiX spike-in).

2.3 Bioinformatics

The raw MiSeq data were converted into FASTQ files using the bcl2fastq program provided by Illumina. The FASTQ files were then demultiplexed using the program Claident v0.2.2015.03.11 [33, 34]. To avoid possible errors resulting from low-quality index sequences, the sequencing reads whose 8-mer index positions included nucleotides with low (< 30) quality scores were discarded in this process. The forward and reverse sequencing reads were then fused with each other using the program PEAR v0.9.6 with a stringent criterion for merging (p = 0.0001).

Among the 11,948,484 reads obtained for ITS1 region, 121,609 were excluded from the subsequent process because their sequences were less than 150 bp or because 10% or more of their nucleotides had low (< 30) quality values. We also discarded potentially chimeric reads using the programs UCHIME v4.2 (*de novo* mode) [35]. In addition, noisy reads were removed by the approach of Li *et al.* [36] with Claident, leaving 10,366,999 reads. The remained reads were clustered with a cutoff sequence similarity of 97% based on a parallelized process of the genome assembler Minimus [37], which also enabled highly accurate clustering of PCR-amplified marker regions, as implemented in Claident. The obtained consensus sequences were then used as operational taxonomic units (OTUs) in the subsequent community ecological analyses. In this clustering process, reads of each sample were clustered beforehand with a cutoff sequence similarity of 98%: the clustered-read membership of the within-sample clustering was used as guide information in order only to accelerate the 97% clustering process. Among the OTUs obtained, we excluded ones whose sequencing reads were less than ten [38] in all samples because their sequences were likely to contain PCR/sequencing errors. After this process, the number of remaining OTUs was 2,886.

For each of the obtained OTUs, taxonomic identification was conducted based on query-centric auto-*k*-nearest-neighbor (QCauto) method [34] and subsequent taxonomic assignment with the lowest common ancestor algorithm [39] using Claident. A benchmark

186 analysis has shown that the combination of the QCauto and LCA algorithms returns the most
187 accurate taxonomic identification results among the existing methods of automated DNA
188 barcoding [34]. Also importantly, the QCauto method is applicable to the DNA barcoding of
189 not only ectomycorrhizal fungi but also diverse clades of endophytic fungi [22]. The QCauto
190 taxonomic assignment was applied to our OTU dataset using the databases obtained by
191 filtering out unreliable sequence entries from the NCBI "nt" database (downloaded from
192 ftp://ftp.ncbi.nlm.nih.gov/ on January 27, 2015) [34]. Among the filtered databases bundled
193 with Claident, we used the "semiall_genus" database, from which *Caenorhabditis*,
194 *Drosophila*, and vertebrate sequences as well as sequences lacking genus-level taxonomic
195 information were discarded [33]. The QCauto query search results with the database were
196 then subjected to the LCA taxonomic assignment (LCA/genus). The default LCA process is
197 very stringent and conservative in that it assigns taxonomic information at a given rank only
198 when the information of all neighborhood sequences are consistent with each other. Therefore,
199 an additional taxonomic assignment was performed by tolerating 5% mismatches among
200 neighborhood sequences (relaxed-LCA/genus) [22]. To facilitate order-level taxonomic
201 identification, we also conducted a QCauto search based on the "semiall_order" filtered
202 database, from which sequences lacking order-level taxonomic information were excluded,
203 and we then applied the relaxed LCA assignment to the search results (relaxed-LCA/order).
204 The overall taxonomic assignment results were obtained by merging the LCA/genus,
205 relaxed-LCA/genus, and relaxed-LCA/order results in this priority order: i.e., results with less
206 stringent settings were not used if they contradicted those with stringent settings [22]. To
207 confirm the results with the QCauto–LCA process, we also performed taxonomic assignment
208 with the UCLUST approach [40] using UNITE ver.7 dynamic database [41] as implemented
209 in QIIME [42].

210 Based on the QCauto–LCA taxonomic assignment results, 965 non-fungal OTUs were
211 excluded from the dataset. We then obtained a sample (row) × fungal OTU (column) data
212 matrix, in which a cell entry indicated the number of the reads of each OTU in each sample.
213 In the matrix, cell entries whose reads were less than 1% of the total read count of each
214 sample were excluded (1%-filtering; figure S1) because those rare entries could represent
215 contamination from soil or among-sample contamination due to "mis-tagging" [43]. The data
216 matrix was then rarefied to 1000 reads per sample using the vegan v2.2-1 package of R v3.2.0
217 (figure S1). 812 and 24 rare OTUs were discarded in the filtering and rarefaction processes,

respectively.

To exclude non-*Fuscospora* root samples from the dataset, the plant *rbcL* and *trnH-psbA* read data were respectively clustered with a cutoff sequence similarity of 99.8%. Ten root samples, which turned out to be the roots of non-*Fuscospora* plants, were then excluded from the dataset. Overall, we obtained a data matrix including 620 root samples and 592 fungal OTUs (data S1 and S2): 58 samples from which the number of sequencing reads were less than 1000 were discarded in the abovementioned processes. Hereafter, we use the word "species" instead of "OTUs" for simplicity, paying careful attention to the fact that OTUs defined with a fixed sequence similarity value do not necessarily represent fungal species. On average, each root sample was colonized by 11.1 fungal species (SD = 3.7; figure S1).

2.4 Symbiont–symbiont network

To reveal the structure of symbiont–symbiont co-occurrence network, we evaluated the extent of the aggregation of fungal symbionts within plant-root samples. For each pair of fungal species, we first calculated the togetherness score (*T* score) [44], which was defined as follows:

$$T = S\,(N + S - R_i - R_j),$$

where N was the total number of root samples examined, R_i and R_j were the total number of the occurrences (root sample counts) of species i and j, and S the number of co-occurrences of species i and j. By using the togetherness score, we performed a randomization test to evaluate the extent of aggregation for each pair of fungal species. In the randomization analysis for each pair of fungal species, the entry of one species was randomized across root samples (100,000 permutations). To evaluate how the observed togetherness was deviated from randomized ones, we calculated standardized togetherness as follows:

$$\text{standardized togetherness} = [T_{observed} - \text{Mean}(T_{randomized})] \,/\, \text{SD}(T_{randomized}),$$

where $T_{observed}$ is the togetherness of the original data, and $\text{Mean}(T_{randomized})$ and $\text{SD}(T_{randomized})$ were the mean and standard deviation of the togetherness scores of randomized data, respectively. In the togetherness analysis, we used the data of the 52 fungal species that occurred in 30 or more root samples (data S3). The results for 1,326 fungal species pairs were

subjected to multiple comparison analysis based on false discovery rate (FDR) [45]. We then drew a symbiont–symbiont co-occurrence network by compiling links between pairs of fungal species that displayed statistically significant (FDR < 0.05) signs of aggregation (togetherness) (data S3). Fungal species within the network was placed using the ForceAtlas2 algorithm [46].

We also evaluated how pairs of fungal species showed mutually segregated distribution across root samples using the checkerboard score (*C* score) [44], which was calculated as follows:

$$C = (R_i - S) \times (R_j - S).$$

For each of the 1,326 fungal species pairs, a randomization analysis of checkerboard scores was conducted (100,000 permutations). Pairs of fungal species with statistically significant (FDR < 0.05) signs of segregation were then indicated on the abovementioned co-occurrence network.

In addition to the togetherness and checkerboard score analyses for the presence/absence dataset format, we also performed analyses of possible symbiont–symbiont associations based on two methods using sequencing-read count information. One used the information of compositional correlations between pairs of species (the sparse correlations for compositional data [SparCC] method [47]) and the other was based on the concept of "conditional independence" between pairs of species (the sparse inverse covariance estimation for ecological association inference (SPIEC-EASI) method [48]). In the SparCC analysis, the threshold of absolute correlation coefficients were set to 0.3 as in a benchmark study comparing SparCC and SPIEC-EASI approaches [48]. In the SPIEC-EASI analysis, the Meinshausen and Bühlmann (MB) algorithm [49] was applied. As these composition-based methods are usually applied to data matrices without rare species [47, 48], the 52 fungal species analyzed in the togetherness/checkerboard tests were screened from the original data matrix (data S1). We also screened samples with sufficient compositional (read-count) information by removing those with less than 5000 sequencing reads. As a result, the input data matrix for the SparCC and SPIEC-EASI analyses consisted of 277 samples and the 52 fungal species (data S1). Those analyses based on sequencing read counts deserve utmost care because they can be more vulnerable to biases resulting from interspecific variation in the

number of ribosomal DNA tandem repeats and compositional biases introduced in PCR-amplification processes than analyses based on presence/absence information [50].

2.5 Symbiont modules

We examined how the symbiont–symbiont co-occurrence network was partitioned into the modules of frequently coexisting fungal species. Modules were detected based on a "data-compression-based" approach using the Infomap algorithm [51], which was known to find network modules the most accurately among available methods [52]. Fungal species composition of each module was inferred based on consensus [53] over 1,000 Infomap runs with the default setting.

By focusing on pairs of fungal species belonging to different modules, we evaluated relationships among the detected modules. Specifically, the ratio of significant aggregation links to possible symbiont–symbiont combinations was calculated as follows:

$$\text{ratio of among-module aggregation} = S_{ij} / N_i \times N_j,$$

where S_{ij} denoted the number of statistically significant (FDR < 0.05) aggregations (togetherness scores) between fungal species in modules i and j, and N_i and N_j represented the number of fungal species in modules i and j, respectively. The ratio of among-module segregation was also calculated in the same way based on the analysis of checkerboard scores.

2.6 Clustering analysis of root sample

In light of the statistical method used in the "enterotyping" of human gut microbiome [10], we conducted the clustering of fungal species compositions of the root samples. For each pair of the root samples, Bray-Curtis β-diversity of fungal species composition was calculated (method S1). Plant root samples were then partitioned into clusters in terms of their fungal species compositions based on the partitioning around medoids (PAM) algorithm of clustering for a given number of clusters [10]. Based on the results with various *a priori* cluster numbers, the optimal number of clusters was estimated with the Calinski-Harabasz index [54]. Nonmetric multidimensional scaling (NMDS) was then performed to visualize the

inferred clusters. In the clustering and NMDS visualization, the vegan, cluster v2.0.1 and clusterSim v.0.44-2 packages of R were used.

2.7 Network hubs

To evaluate the topological properties of each fungal species within the symbiont–symbiont co-occurrence network, we calculated betweenness [55, 56] centrality. Fungal species with high betweenness are expected to play important "topological roles" in interconnecting pairs of other fungal species in the symbiont–symbiont co-occurrence network [55, 56]. The obtained betweenness values were *z*-standardized (zero-mean; unit-variance). In addition to the betweeness analysis, topological roles in interconnecting species in different modules (participation coefficient [55, 57]) and the number of links with species in the same module (within-module degree) were calculated. The former can vary from 0 (species linked only with species in the same modules) to 1 (species interacting indiscriminately with species in all modules), while the latter was *z*-standardized.

2.8 Spatial scales of sampling

Because the roots analyzed were collected randomly at 1-m intervals within the forest, our samples as a whole may have included those from the same *Fuscospora* individuals. Thus, we conducted an additional analysis in which each root sample was expected to represent a plant individual. As sampling was conducted in a mature forest with closed canopy, roots collected at 5-m intervals were possibly those of different host plant individuals. Therefore, we divided the 1-m interval full data into five partial datasets, each of which consisted of the root samples collected at 5-m intervals (data S4). For each of the five partial dataset, the randomization analysis of the togetherness and checkerboard scores were performed for each pair of fungal species. Fungal species that occurred in 10 or more root samples in each partial dataset were subjected to the analysis.

3. Results

3.1 Architecture of the symbiont–symbiont co-occurrence network

The symbiont–symbiont co-occurrence network in the *Fuscospora* forest displayed highly organized structure in terms of the sets of fungal species that frequently coexisted within the narrow space of host root systems (figure 1). The network representing statistically significant aggregation patterns was partitioned into five modules (excluding modules containing only one species) and each of the modules included fungi in phylogenetically diverse lineages (figures 1 and 2; see also figure S2). A complementary network analysis based on checkerboard scores further indicated that fungi in different network modules often showed segregated patterns (figure 1*c*). In particular, fungi in the module 1 (module group A) seldom co-occurred with those in the modules 2–5 (module group B), while fungi in the latter three modules frequently coexisted within host root systems (figures 1 and 2).

There were some characteristics in the taxonomic compositions of the module groups (table 1; table S1). First, both module groups included ectomycorrhizal fungi in Cortinariaceae as well as fungi in the ascomycete order Helotiales, which were known to include endophytic and ectomycorrhizal lineages [58] (table 1). Second, other than Helotiales fungi, the module group A was represented by fungi in the genus *Oidiodendron*, while the module group B was dominated by a fungus in the ectomycorrhizal genus *Cenococcum* (table 1). Third, whereas some *Oidiodendron* fungi were included not only in the module group A but also in the module group B, *Cenococcum* appeared only in the module group B (table S1).

Additional analyses based on sequencing-read count information (the SparCC and SPIEC-EASI analyses) further indicated the existence of those modules or module groups (figure 3). Meanwhile, the number of links connecting fungal species was fewer in the SparCC/SPIEC-EASI analyses than that in the togetherness/checkerboard analyses (cf. figures 1 and 3). As a result, 14 of the 52 fungal species examined did not have links, and the module or module groups (figure 1) appeared as discrete clusters (figure 3*a*, *b*).

3.2 Clustering of fungal symbiont communities

The characteristic structure of the symbiont–symbiont co-occurrence network was reflected in the formation of fungal community type in the *Fuscospora* host plant. That is, fungal symbiont composition of terminal root samples in the forest was partitioned into two

semi-discrete statistical clusters (figure 4*a*, *b*; figure S3). The two clusters corresponded to the compartmentalized pattern of the symbiont–symbiont network: i.e., one cluster consisted of root samples frequently colonized by fungi in the module group A, while the other represented samples harboring fungi in the module group B at high frequency (figure 4*c*). Although a small fraction of samples hosted both module groups of fungi at comparative proportions, the fungal composition of most root samples was biased toward colonization by either of the fungal module groups (figure 4*d*). An additional analysis showed that there was a spatially auto-correlated pattern in the distribution of fungal community clusters within the forest (figure 4*e*; see also figure S4).

3.3 Network hubs within the symbiont–symbiont co-occurrence network

We then focused on how each fungal species were embedded within the symbiont–symbiont co-occurrence network and found that several fungal species in the community were placed at the core of the network (figure 5). Some of those "network hub [55, 59]" species interlinked fungi in different modules within the symbiont–symbiont co-occurrence network [e.g., an endophytic fungus in Herpotrichiellaceae ("23_Herpotrichiellaceae")], while others interconnected most fungal species within each module [e.g., an ectomycorrhizal fungus in the genus *Cenococcum* ("2_Cenococcum")] (figures 1 and 5*a*, *b*). Although generalist fungi that occurred in most samples could be the former type of network hubs (hereafter, "inter-module hubs"), the most frequently-observed fungi (fungi observed from more than 200 samples) within the dataset (figure 5*c*) had the latter type of topological characteristics (hereafter, "within-module hubs") (figure 5*a*). When the sample counts of each fungal species (i.e., the number of root samples from which each species was detected; figure 5*c*) was controlled, inter-module hubs were distinguished from within-module hubs as well as peripheral (rarer) species in the network (figure 5*d*).

3.4 Spatial scales of sampling

In the analysis based on the 5-m interval partial datasets, the number of fungal pairs that displayed statistically significant (FDR < 0.05) signs of aggregation/segregation was inevitably reduced due to the decreased sample size in the partial datasets (figure S5; data S4).

However, many of the core symbiont–symbiont aggregation/segregation patterns found in the full-data analysis (figure 1) were reproduced in the additional analysis (figure S5; data S4), although care should be paid to the possibility that the 5-m interval partial datasets could still include some samples from the same host plant individuals.

4. DISCUSSION

There are some potential mechanisms that can generate the observed differentiation of fungal symbiont compositions among host plant samples. For example, fungi in each module group (figure 2*a*) may share ecological niches [19], adapting to the same fine-scale environments in soil [38]. The spatial autocorrelation observed in the distribution of fungal community clusters within the forest (figure 4*e*) might reflect the suspected effects of such environmental factors.

Another important possibility, albeit not mutually exclusive with the former one, is that the observed semi-discrete community structures are organized mainly by direct symbiont–symbiont interactions. There has been clear experimental evidence that ectomycorrhizal fungal species compete for space within host root systems and that they strongly prevent the colonization of late comers through "priority effects" [15, 16, 60]. Such competitive exclusion mechanisms have been reported not only between ectomycorrhizal fungi but also between arbuscular mycorrhizal fungi [60]. In contrast to those negative interactions between fungal symbionts, pairs of fungi in facilitative interactions, especially those showing functional complementarity, are expected to coexist within the same terminal root tissue, displaying more aggregated patterns than expected by chance [18]. In this respect, the result that each module group included both ectomycorrhizal and endophytic fungi (figures 1*c* and 2) is interesting. This study was designed to screen for the signs of potential interactions between symbionts and revealed how diverse phylogenetic and functional groups of fungi constitute modules in a symbiont–symbiont co-occurrence network. Although the relative contributions of soil-environmental niche partitioning/sharing and direct interspecific interactions to the observed community patterns should be examined in future experimental studies, the analytical framework shown here provides a basis for understanding the mechanisms by which (semi-)discrete symbiont community structures are organized at the

network level.

In general, the presence of alternative community compositions is represented by the term “alternative stable state” [61, 62]. Conceptually, there are two different contexts defining alternative stable states [63]. In one definition, shifts between alternative community structures occur in response to changes in state variables (e.g., population densities of respective species) [64, 65], while in the other definition, they occur as a consequence of changes in environmental parameters (e.g., host nutritional conditions) [66, 67]. Although the former definition is frequently used in recent studies of community ecology [65], the latter definition would attract more attention in the context of applied microbiology, whose focus is on the possible relationships between microbiome structure and host physiological states [5, 11, 12, 68]. As symbiont community compositions can be not only the signs of host states but also the determinants of hosts’ health [14, 69, 70], it should be essential to investigate whether alternative structures of root-associated fungal communities are equal or different in their effects to plants’ physiology and performance.

The observed difference in taxonomic compositions between the module groups A and B (table 1) is of particular interest in this point. Although both module groups included Cortinatiaceae and Helotiales fungi as major components, the module group A was represented by *Oidiodendron* fungi, which have been known as saprotorophic or ericoid mycorrhizal fungi [71]. In contrast, the module group B was dominated by a fungus in a well-characterized ectomycorrhizal genus, *Cenococcum*, which surrounds host root-tips with heavily melanized mycelia [72] and produces antibiotics against pathogenic bacteria [73]. Given the ambiguous symbiotic status of *Oidiodendron* and the unique ectomycorrhizal feature of *Cenococcum* [74], the two fungal module groups observed in this study (figure 2; table 1) may be playing distinct ecological roles in the *F. cliffortioides* population.

Another future research direction is illuminated by the working hypothesis that a small fraction of symbiont species can play essential roles in the assembly of plant-root microbiomes. The existence of topological hubs in symbiont–symbiont networks leads to the hypothesis that a small fraction of microbes play predominant roles in the organization of symbiont community structure (or rhizotype). Specifically, the presence of within-module hub species may facilitate the subsequent root colonization of other mycorrhizal, endophytic and pathogenic fungal species belonging to the same modules or module groups, while it may

prevent the colonization of fungi in other module groups (see studies examining possible fungus-to-fungus interactions within host root systems [15, 60, 75, 76]). Accordingly, the rhizotype of plant root system might be determined, in large part, depending on which hub species first colonize the root tissue [60, 77]. Given that potential within-module hubs had the highest sample counts (i.e., the number of samples from which they were observed) in our data (figure 5*c*), they may actually colonize host tissue earlier than others, organizing microbiome structure within the hosts through priority effects. Meanwhile, inter-module hubs (figure 5*d*), albeit absent in the analyses based on sequencing-read count data (figure 3), may also play important roles in, for instance, the switching of alternative rhizotypes. However, our knowledge of such shifts among alternative symbiont community structures has still been limited.

Although the observed patterns in the symbiont–symbiont co-occurrence network allow us to raise some intriguing hypotheses on microbiome assembly processes, our results are based on an analysis of only one monodominant forest, thereby providing limited chances for extrapolating the above discussion to other forest, grassland or agricultural ecosystems. In addition, the fully observational approach of our study precludes explicit testing of the existence of alternative stable states (or rhizotypes) and possible mechanisms underlying within-host dynamics of fungal symbiont communities. Also importantly, the use of molecular operational taxonomic units as units of statistical analysis has been subject to continuing methodological challenges in microbiology [4, 78]. Nonetheless, we herein showed how to reconstruct the networks of potential symbiont-to-symbiont interactions based on field sampling and high-throughput sequencing. Moreover, the working hypothesis that a small number of “fixer” species within a symbiont–symbiont co-occurrence network regulate within-host microbial communities deserves attention in both basic and applied ecology, providing a basis for future experimental and theoretical studies.

Overall, analysis of symbiont–symbiont networks is crucial in finding hub species, whose compatibility with plant genotypes and physiological conditions is likely to be the key to understanding the mechanisms that organize symbiont community structures. Thus, even the virtually complex dynamics of communities involving hundreds or more of root-associated microbial species may be reduced to the genetics or ecology of those hub species [79], if the architecture of symbiont–symbiont networks is properly estimated. Specifically, we may be

able to manipulate plant-associated microbial communities by inoculating plant seedlings with hub microbial species or optimizing genetic compatibility between host plants and those hub microbes. More observational and experimental studies targeting other microbial groups (e.g., bacteria [80]) in various ecosystems are awaited to address the validity of such reductionistic control of plant-associated microbiomes.

Data accessibility. The accession number of the DDBJ Sequence Read Archive: DRA003730. The data matrices supporting this article have been uploaded as part of the electric supplementary material.

Authors' contributions. H.T. designed the research. H.T. and H.S.I. performed fieldwork. H.T., S.Y. and T.H. conducted molecular experiments. H.T. and A.S.T. analyzed the data. H.T. wrote the paper.

Competing interests. We declare no competing interests.

Funding. This work was financially supported by JSPS KAKENHI Grant (No. 26711026) and the Funding Program for Next Generation World-Leading Researchers of Cabinet Office, the Government of Japan (GS014) to H.T.. H.S.I. was supported by JSPS KAKENHI Grant (No. 23405006).

Acknowledgements. We thank Yukuto Sato and Atsushi Nagano for their advice on next-generation sequencing and Minato Kodama for her support in molecular experiments.

References

1. Selosse, M-A, Strullu-Derrien, C, Martin, FM, Kamoun, S & Kenrick, P. 2015 Plants, fungi and oomycetes: a 400-million year affair that shapes the biosphere. *New Phytol.* **206**, 501-506.

2. van der Heijden, MG, Martin, FM, Selosse, MA & Sanders, IR. 2015 Mycorrhizal ecology and evolution: the past, the present, and the future. *New Phytol.* **205**, 1406-1423.

3. Bever, JD. 2003 Soil community feedback and the coexistence of competitors: conceptual frameworks and empirical tests. *New Phytol.* **157**, 465-473.

4. Toju, H, Guimarães Jr, PR, Olesen, JM & Thompson, JN. 2014 Assembly of complex plant–fungus networks.

513 *Nature Commun.* **5**, 5273.

514 5. Berendsen, RL, Pieterse, CM & Bakker, PA. 2012 The rhizosphere microbiome and plant health. *Trends Plant*
515 *Sci.* **17**, 478-486.

516 6. Ikeda, S, Okubo, T, Anda, M, Nakashita, H, Yasuda, M, Sato, S, Kaneko, T, Tabata, S, Eda, S & Momiyama,
517 A. 2010 Community-and genome-based views of plant-associated bacteria: plant–bacterial interactions in
518 soybean and rice. *Plant Cell Physiol.* **51**, 1398-1410.

519 7. Edwards, J, Johnson, C, Santos-Medellín, C, Lurie, E, Podishetty, NK, Bhatnagar, S, Eisen, JA & Sundaresan,
520 V. 2015 Structure, variation, and assembly of the root-associated microbiomes of rice. *Proc. Natl. Acad. Sci.*
521 *USA* **112**, E911-E920.

522 8. Lundberg, DS, Lebeis, SL, Paredes, SH, Yourstone, S, Gehring, J, Malfatti, S, Tremblay, J, Engelbrektson, A,
523 Kunin, V & Del Rio, TG. 2012 Defining the core *Arabidopsis thaliana* root microbiome. *Nature* **488**, 86-90.

524 9. Tedersoo, L, Bahram, M, Põlme, S, Kõljalg, U, Yorou, NS, Wijesundera, R, Ruiz, LV, Vasco-Palacios, AM,
525 Thu, PQ & Suija, A. 2014 Global diversity and geography of soil fungi. *Science* **346**, 1256688.

526 10. Arumugam, M, Raes, J, Pelletier, E, Le Paslier, D, Yamada, T, Mende, DR, Fernandes, GR, Tap, J, Bruls, T
527 & Batto, J-M. 2011 Enterotypes of the human gut microbiome. *Nature* **473**, 174-180.

528 11. Lozupone, CA, Stombaugh, JI, Gordon, JI, Jansson, JK & Knight, R. 2012 Diversity, stability and resilience
529 of the human gut microbiota. *Nature* **489**, 220-230.

530 12. Qin, J, Li, Y, Cai, Z, Li, S, Zhu, J, Zhang, F, Liang, S, Zhang, W, Guan, Y & Shen, D. 2012 A
531 metagenome-wide association study of gut microbiota in type 2 diabetes. *Nature* **490**, 55-60.

532 13. Faust, K & Raes, J. 2012 Microbial interactions: from networks to models. *Nature Rev. Microbiol.* **10**,
533 538-550.

534 14. Fukuda, S, Toh, H, Hase, K, Oshima, K, Nakanishi, Y, Yoshimura, K, Tobe, T, Clarke, JM, Topping, DL &
535 Suzuki, T. 2011 Bifidobacteria can protect from enteropathogenic infection through production of acetate.
536 *Nature* **469**, 543-547.

537 15. Kennedy, PG, Peay, KG & Bruns, TD. 2009 Root tip competition among ectomycorrhizal fungi: are priority
538 effects a rule or an exception? *Ecology* **90**, 2098-2107.

539 16. Koide, RT, Xu, B, Sharda, J, Lekberg, Y & Ostiguy, N. 2005 Evidence of species interactions within an
540 ectomycorrhizal fungal community. *New Phytol.* **165**, 305-316.

541 17. Bakker, MG, Schlatter, DC, Otto-Hanson, L & Kinkel, LL. 2014 Diffuse symbioses: roles of plant–plant,

542 plant–microbe and microbe–microbe interactions in structuring the soil microbiome. *Mol. Ecol.* **23**, 1571-1583.

543 18. Yamamoto, S, Sato, H, Tanabe, AS, Hidaka, A, Kadowaki, K & Toju, H. 2014 Spatial segregation and
544 aggregation of ectomycorrhizal and root-endophytic fungi in the seedlings of two *Quercus* species. *PLOS ONE* **9**,
545 e96363.

546 19. Dickie, IA. 2007 Host preference, niches and fungal diversity. *New Phytol.* **174**, 230-233.

547 20. Toju, H, Guimarães, PR, Jr, Olesen, JM & Thompson, JN. 2015 Below-ground plant–fungus network
548 topology is not congruent with above-ground plant–animal network topology. *Sci. Adv.* **1**, e1500291.

549 21. Newsham, KK. 2011 A meta-analysis of plant responses to dark septate root endophytes. *New Phytol.* **190**,
550 783-793.

551 22. Toju, H, Yamamoto, S, Sato, H, Tanabe, AS, Gilbert, GS & Kadowaki, K. 2013 Community composition of
552 root-associated fungi in a *Quercus*-dominated temperate forest: "codominance"of mycorrhizal and
553 root - endophytic fungi. *Ecol. Evol.* **3**, 1281-1293.

554 23. Heenan, PB & Smissen, RD. 2013 Revised circumscription of *Nothofagus* and recognition of the segregate
555 genera *Fuscospora*, *Lophozonia*, and *Trisyngyne* (Nothofagaceae). *Phytotaxa* **146**, 1-31.

556 24. Thompson, JN. 2005 *The geographic mosaic of coevolution*. Chicago, The University of Chicago Press.

557 25. Sato, H & Murakami, N. 2008 Reproductive isolation among cryptic species in the ectomycorrhizal genus
558 *Strobilomyces*: population-level CAPS marker-based genetic analysis. *Mol. Phyl. Evol.* **48**, 326-334.

559 26. White, TJ, Bruns, T, Lee, S & Taylor, J. 1990 Amplification and direct sequencing of fungal ribosomal RNA
560 genes for phylogenetics. In *PCR protocols: A guide to methods and applications* (eds. M. Innis, D. Gelfand, J.
561 Sninsky & T. White), pp. 315-322. San Diego, Academic Press.

562 27. Lundberg, DS, Yourstone, S, Mieczkowski, P, Jones, CD & Dangl, JL. 2013 Practical innovations for
563 high-throughput amplicon sequencing. *Nature Methods* **10**, 999-1002.

564 28. Toju, H, Tanabe, AS, Yamamoto, S & Sato, H. 2012 High-coverage ITS primers for the DNA-based
565 identification of ascomycetes and basidiomycetes in environmental samples. *PLOS ONE* **7**, e40863.

566 29. Hamady, M, Walker, JJ, Harris, JK, Gold, NJ & Knight, R. 2008 Error-correcting barcoded primers for
567 pyrosequencing hundreds of samples in multiplex. *Nature Methods* **5**, 235-237.

568 30. Toju, H, Yamamoto, S, Sato, H & Tanabe, AS. 2013 Sharing of diverse mycorrhizal and root-endophytic
569 fungi among plant species in an oak-dominated cool–temperate forest. *PLOS ONE* **8**, e78248.

570 31. Sang, T, Crawford, D & Stuessy, T. 1997 Chloroplast DNA phylogeny, reticulate evolution, and
571 biogeography of *Paeonia* (Paeoniaceae). *Amer. J. Bot.* **84**, 1120-1120.

572 32. Tate, JA & Simpson, BB. 2003 Paraphyly of *Tarasa* (Malvaceae) and diverse origins of the polyploid
573 species. *Syst. Bot.* **28**, 723-737.

574 33. Tanabe, AS. 2015 *Claident v0.2.2015.03.11, a software distributed by author at*
575 http://www.fifthdimension.jp/.

576 34. Tanabe, AS & Toju, H. 2013 Two new computational methods for universal DNA barcoding: A benchmark
577 using barcode sequences of bacteria, archaea, animals, fungi, and land plants. *PLOS ONE* **8**, e76910.

578 35. Edgar, RC, Haas, BJ, Clemente, JC, Quince, C & Knight, R. 2011 UCHIME improves sensitivity and speed
579 of chimera detection. *Bioinformatics* **27**, 2194-2200.

580 36. Li, W, Fu, L, Niu, B, Wu, S & Wooley, J. 2012 Ultrafast clustering algorithms for metagenomic sequence
581 analysis. *Brief. Bioinfo.*, bbs035.

582 37. Sommer, DD, Delcher, AL, Salzberg, SL & Pop, M. 2007 Minimus: a fast, lightweight genome assembler.
583 *BMC Bioinfo.* **8**, 64.

584 38. Peay, KG, Russo, SE, McGuire, KL, Lim, Z, Chan, JP, Tan, S & Davies, SJ. 2015 Lack of host specificity
585 leads to independent assortment of dipterocarps and ectomycorrhizal fungi across a soil fertility gradient. *Ecol.*
586 *Lett.* **18**, 807-816.

587 39. Huson, DH, Auch, AF, Qi, J & Schuster, SC. 2007 MEGAN analysis of metagenomic data. *Genome Res.* **17**,
588 377-386.

589 40. Edgar, RC. 2010 Search and clustering orders of magnitude faster than BLAST. *Bioinformatics* **26**,
590 2460-2461.

591 41. Abarenkov, K, Henrik Nilsson, R, Larsson, KH, Alexander, IJ, Eberhardt, U, Erland, S, Høiland, K, Kjøller,
592 R, Larsson, E & Pennanen, T. 2010 The UNITE database for molecular identification of fungi–recent updates
593 and future perspectives. *New Phytol.* **186**, 281-285.

594 42. Caporaso, JG, Kuczynski, J, Stombaugh, J, Bittinger, K, Bushman, FD, Costello, EK, Fierer, N, Pena, AG,
595 Goodrich, JK & Gordon, JI. 2010 QIIME allows analysis of high-throughput community sequencing data.
596 *Nature Methods* **7**, 335-336.

597 43. Philippe, E, Franck, L & Jan, P. 2015 Accurate multiplexing and filtering for high-throughput
598 amplicon-sequencing. *Nuc. Acid. Res.*, gkv107.

599 44. Stone, L & Roberts, A. 1992 Competitive exclusion, or species aggregation? *Oecologia* **91**, 419-424.

600 45. Benjamini, Y & Hochberg, Y. 1995 Controlling the false discovery rate: a practical and powerful approach
601 to multiple testing. *J. R. Stat. Soc. Ser. B.* **57**, 289-300.

602 46. Jacomy, M, Venturini, T, Heymann, S & Bastian, M. 2014 ForceAtlas2, a continuous graph layout algorithm
603 for handy network visualization designed for the Gephi software. *PLOS ONE* **9**, e98679.

604 47. Friedman, J & Alm, EJ. 2012 Inferring correlation networks from genomic survey data. *PLOS Comp. Biol.* **8**,
605 e1002687.

606 48. Kurtz, ZD, Mueller, CL, Miraldi, ER, Littman, DR, Blaser, MJ & Bonneau, RA. 2015 Sparse and
607 compositionally robust inference of microbial ecological networks. *PLOS Comp. Biol.* **11**, e1004226.

608 49. Meinshausen, N & Bühlmann, P. 2006 High-dimensional graphs and variable selection with the lasso. *Ann.*
609 *Stat.* **34**, 1436-1462.

610 50. Toju, H. 2015 High-throughput DNA barcoding for ecological network studies. *Popul. Ecol.* **57**, 37-51.

611 51. Rosvall, M & Bergstrom, CT. 2011 Multilevel compression of random walks on networks reveals
612 hierarchical organization in large integrated systems. *PLOS ONE* **6**, e18209.

613 52. Orman, GK, Labatut, V & Cherifi, H. 2012 Comparative evaluation of community detection algorithms: a
614 topological approach. *J. Stat. Mech. Theor. Exper.* **2012**, P08001.

615 53. Lancichinetti, A & Fortunato, S. 2012 Consensus clustering in complex networks. *Sci. Rep.* **2**, 336.

616 54. Caliński, T & Harabasz, J. 1974 A dendrite method for cluster analysis. *Commun. Stat.* **3**, 1-27.

617 55. Guimera, R, Mossa, S, Turtschi, A & Amaral, LN. 2005 The worldwide air transportation network:
618 Anomalous centrality, community structure, and cities' global roles. *Proc. Natl. Acad. Sci. USA* **102**, 7794-7799.

619 56. Freeman, LC. 1977 A set of measures of centrality based on betweenness. *Sociometry* **40**, 35-41.

620 57. Olesen, JM, Bascompte, J, Dupont, YL & Jordano, P. 2007 The modularity of pollination networks. *Proc.*
621 *Natl. Acad. Sci. USA* **104**, 19891-19896.

622 58. Tedersoo, L, Pärtel, K, Jairus, T, Gates, G, Põldmaa, K & Tamm, H. 2009 Ascomycetes associated with
623 ectomycorrhizas: molecular diversity and ecology with particular reference to the Helotiales. *Env. Microbiol.* **11**,
624 3166-3178.

625 59. Newman, M. 2010 *Networks: an introduction*. Oxford, Oxford University Press.

626 60. Werner, GD & Kiers, ET. 2015 Order of arrival structures arbuscular mycorrhizal colonization of plants.
627 *New Phytol.* **205**, 1515-1524.

628 61. Lewontin, RC. 1969 The meaning of stability. *Brookhaven Symp. Biol.* **22**, 13-23.

629 62. Schröder, A, Persson, L & De Roos, AM. 2005 Direct experimental evidence for alternative stable states: a
630 review. *Oikos* **110**, 3-19.

631 63. Beisner, BE, Haydon, DT & Cuddington, K. 2003 Alternative stable states in ecology. *Front. Ecol. Env.* **1**,
632 376-382.

633 64. Drake, JA. 1991 Community-assembly mechanics and the structure of an experimental species ensemble. *Am.*
634 *Nat.* **137**, 1-26.

635 65. Fukami, T & Nakajima, M. 2011 Community assembly: alternative stable states or alternative transient
636 states? *Ecol. Lett.* **14**, 973-984.

637 66. May, RM. 1977 Thresholds and breakpoints in ecosystems with a multiplicity of stable states. *Nature* **269**,
638 471-477.

639 67. Scheffer, M, Carpenter, S, Foley, JA, Folke, C & Walker, B. 2001 Catastrophic shifts in ecosystems. *Nature*
640 **413**, 591-596.

641 68. Yatsunenko, T, Rey, FE, Manary, MJ, Trehan, I, Dominguez-Bello, MG, Contreras, M, Magris, M, Hidalgo,
642 G, Baldassano, RN & Anokhin, AP. 2012 Human gut microbiome viewed across age and geography. *Nature* **486**,
643 222-227.

644 69. Foster, JA & Neufeld, K-AM. 2013 Gut–brain axis: how the microbiome influences anxiety and depression.
645 *Trends Neurosci.* **36**, 305-312.

646 70. Delzenne, NM, Neyrinck, AM, Bäckhed, F & Cani, PD. 2011 Targeting gut microbiota in obesity: effects of
647 prebiotics and probiotics. *Nature Rev. Endocr.* **7**, 639-646.

648 71. Rice, AV & Currah, RS. 2005 *Oidiodendron*: A survey of the named species and related anamorphs of
649 Myxotrichum. *Studies Mycol.* **53**, 83-120.

650 72. Fernandez, CW & Koide, RT. 2013 The function of melanin in the ectomycorrhizal fungus *Cenococcum*
651 *geophilum* under water stress. *Fungal Ecol.* **6**, 479-486.

652 73. Krywolap, GN, Grand, LF & Casida Jr, L. 1964 The natural occurrence of an antibiotic in the mycorrhizal
653 fungus *Cenococcum graniforme*. *Can. J. Microbiol.* **10**, 323-328.

654 74. Marx, DH. 1972 Ectomycorrhizae as biological deterrents to pathogenic root infections. *Ann. Rev.*
655 *Phytopathol.* **10**, 429-454.

656 75. Kennedy, PG, Bergemann, SE, Hortal, S & Bruns, TD. 2007 Determining the outcome of field-based
657 competition between two *Rhizopogon* species using real-time PCR. *Mol. Ecol.* **16**, 881-890.

658 76. Kennedy, PG & Bruns, TD. 2005 Priority effects determine the outcome of ectomycorrhizal competition
659 between two *Rhizopogon* species colonizing *Pinus muricata* seedlings. *New Phytol.* **166**, 631-638.

660 77. Peay, KG, Belisle, M & Fukami, T. 2011 Phylogenetic relatedness predicts priority effects in nectar yeast
661 communities. *Proc. R. Soc. Ser. B* **279**, 749-758.

662 78. Nilsson, RH, Kristiansson, E, Ryberg, M, Hallenberg, N & Larsson, K-H. 2008 Intraspecific ITS variability
663 in the kingdom Fungi as expressed in the international sequence databases and its implications for molecular
664 species identification. *Evol. Bioinformatics* **4**, 193-201.

665 79. Whitham, TG, Bailey, JK, Schweitzer, JA, Shuster, SM, Bangert, RK, LeRoy, CJ, Lonsdorf, EV, Allan, GJ,
666 DiFazio, SP & Potts, BM. 2006 A framework for community and ecosystem genetics: from genes to ecosystems.
667 *Nature Rev. Genetics* **7**, 510-523.

668 80. Bonfante, P & Anca, I-A. 2009 Plants, mycorrhizal fungi, and bacteria: a network of interactions. *Ann. Rev.*
669 *Microbiol.* **63**, 363-383.

670

671 **Electric supplementary materials**

672 **Method S1**. Supplementary methods for the clustering analysis.

673 **Figure S1.** Rarefaction curves of the sequencing reads.

674 **Figure S2.** Composition of the 592 fungal species.

675 **Figure S3.** Symbiont–symbiont networks estimated based on the 5-m interval partial datasets.

676 **Figure S4.** Clustering analysis based on the 592-fungus full dataset.

677 **Table S1.** Fungi that appeared in 30 or more samples.

678 **Data S1**. Data matrix and fungal taxonomic information.

679 **Data S2.** ITS1 sequences of the fungi analyzed.

680 **Data S3.** Results and data of the aggregation/segregation analysis.

Data S4. Results of togetherness and checkerboard analysis for 5-m interval partial datasets.

683

684 **Table 1. Major fungal species in the two module groups.** For each of the module group A
685 (module 1) and B (modules 2–5) (figure 2), top 10 fungal species with highest sample counts
686 (the number of root samples) are shown. The information of the lowest taxonomic rank
687 assigned by the UCLUST algorithm with UNITE ver.7 dynamic database is also shown with
688 the results with the QCauto–LCA approach.

689

OTU	Module	*N*samples	Phylum	Class	Order	Family	Genus	Functional group	UNITE
F3	A (1)	245	Ascomycota	Leotiomycetes	Helotiales			Unknown	Dermateaceae
F4	A (1)	237	Ascomycota	Leotiomycetes		Myxotrichaceae	Oidiodendron	Unknown	*Oidiodendron*
F5	A (1)	235	Ascomycota	Leotiomycetes		Myxotrichaceae	Oidiodendron	Unknown	*Oidiodendron*
F6	A (1)	222	Ascomycota	Leotiomycetes		Myxotrichaceae	Oidiodendron	Unknown	*Oidiodendron*
F7	A (1)	210	Basidiomycota	Agaricomycetes	Agaricales	Cortinariaceae	Cortinarius	Ectomycorrhizal	*Cortinarius*
F8	A (1)	207	Ascomycota	Leotiomycetes	Helotiales			Unknown	Helotiales
F9	A (1)	161	Ascomycota	Leotiomycetes		Myxotrichaceae	Oidiodendron	Unknown	*Oidiodendron*
F11	A (1)	144	Ascomycota	Leotiomycetes	Helotiales			Unknown	Unassigned
F12	A (1)	134			Mortierellales	Mortierellaceae	Mortierella	Unknown	*Mortierella*
F15	A (1)	114	Ascomycota	Leotiomycetes	Helotiales			Unknown	Unassigned
F1	B (3)	275	Ascomycota	Leotiomycetes	Helotiales			Unknown	Helotiales
F2	B (2)	270	Ascomycota	Dothideomycetes		Gloniaceae	Cenococcum	Ectomycorrhizal	*Cenococcum*
F10	B (2)	159	Ascomycota	Leotiomycetes	Helotiales			Unknown	Helotiales
F13	B (3)	117	Ascomycota	Eurotiomycetes	Chaetothyriales	Herpotrichiellaceae	Cladophialophora	Unknown	*Cladophialophora*
F14	B (2)	114	Ascomycota	Leotiomycetes	Helotiales	Dermateaceae	Pezicula	Unknown	Dermateaceae
F18	B (2)	98	Ascomycota	Leotiomycetes	Helotiales			Unknown	Helotiales
F20	B (2)	87	Basidiomycota	Agaricomycetes	Agaricales	Cortinariaceae		Ectomycorrhizal	*Cortinarius*
F22	B (5)	77	Ascomycota	Leotiomycetes	Helotiales			Unknown	Helotiales
F24	B (2)	64	Ascomycota					Unknown	Unassigned
F25	B (2)	63	Ascomycota	Leotiomycetes	Helotiales			Unknown	Helotiales

690

691

692 **Figure Captions**

693 **Figure 1.** Symbiont–symbiont co-occurrence network. (*a*) Scores representing the extent of
694 aggregation of fungal symbionts within host root samples. For each pair of fungal species, a
695 togetherness score was examined in a randomization analysis to evaluate aggregated
696 distribution (100,000 permutations). Multiple comparison was performed based on false
697 discovery rate (FDR). (*b*) Scores representing the extent of segregation of fungal symbionts
698 within host root samples. For each pair of fungal species, a checkerboard score was examined
699 in a randomization analysis to evaluate segregated distribution (100,000 permutations). (*c*)
700 Network of aggregated and segregated patterns. Fungal species are linked by the lines
701 indicating statistically significant (FDR < 0.05) aggregation (blue) and segregation (red). The
702 thickness of links is proportional to standardized togetherness or checkerboard scores. The
703 circles representing fungal species (yellow, ectomycorrhizal fungi; gray, fungi with unknown
704 functions) are placed based on the aggregation patterns with the ForceAtlas2 algorithm. The
705 outer parts of the circles represent fungal taxonomy (brown, Ascomycota; green;
706 Basidiomycota; white, unidentified).

707

708 **Figure 2.** Modules within the symbiont–symbiont network. (*a*) Modules and fungal species.
709 The symbiont–symbiont co-occurrence network (i.e., the network indicated by blue lines in
710 figure 1*c*) was partitioned into statistical modules, which represented link-dense assemblages
711 of fungal species. (*b*) Among-module aggregation patterns. The thickness of the links
712 between modules indicates the extent to which fungal species in each pair of modules
713 co-occur within the same root sample. The size of the circles represents the number of fungal
714 species in the modules. (*c*) Among-module segregation patterns. The thickness of the links
715 between modules indicates the extent to which fungal species in each pair of modules display
716 segregated distribution across root samples.

717

718 **Figure 3.** Symbiont–symbiont network patterns analyzed with sequencing read information.
719 (*a*) SparCC analysis for symbiont–symbiont aggregation. Pairs of fungal species with
720 aggregated patterns are linked with each other. Color of circles represents network modules
721 identified in figure 2. (*b*) SPIEC-EASI analysis for symbiont–symbiont aggregation. (*c*)

SparCC analysis for symbiont–symbiont segregation. (*d*) SPIEC-EASI analysis for symbiont–symbiont segregation.

Figure 4. Clusters in the fungal community structure of root samples. (*a*) Number of statistical clusters in the fungal community data of the root samples. The number of clusters was estimated to be two based on the analysis with the Calinski-Harabasz index. (*b*) Nonmetric multidimensional scaling of the fungal community of the root samples. (*c*) Correspondence between fungal module groups and the clusters of the root samples. A bar indicates the mean rate of colonization by fungal species in each module group (mean ± SEM). Welch's test was performed for each cluster. (*d*) Fungal colonization profiles of the root-sample clusters. For each root sample, the mean rate of colonization by fungal species in the module groups A (horizontal axis) and B (vertical axis) is shown. The size of circles represents the number of root samples. (*e*) Distribution of root-sample clusters within the studied forest. Sampling points placed at 1-m intervals along a mountain trail are shown with the root-sample clusters of the collected samples.

Figure 5. Hub fungal species within the symbiont–symbiont network. (*a*) Betweenness centrality metric depicting the topological properties of respective fungal species. Fungal species with high betweenness scores interconnect other fungal species in the symbiont–symbiont co-occurrence network. (*b*) Among- and within-module connectivity. For each fungal species, topological roles in interconnecting species in different modules (participation coefficient) and the number of links with species in the same module (within-module degree) are shown. The color of symbols represents the betweenness centrality of each fungal species (*a*). (*c*) Number of root samples from which each fungal species was detected. (*d*) Standardization of betweenness centrality by the number of samples. Betweenness centrality (*a*) was divided by the number of samples from in which each fungal species occurred (*c*). The obtained values were *z*-standardized.

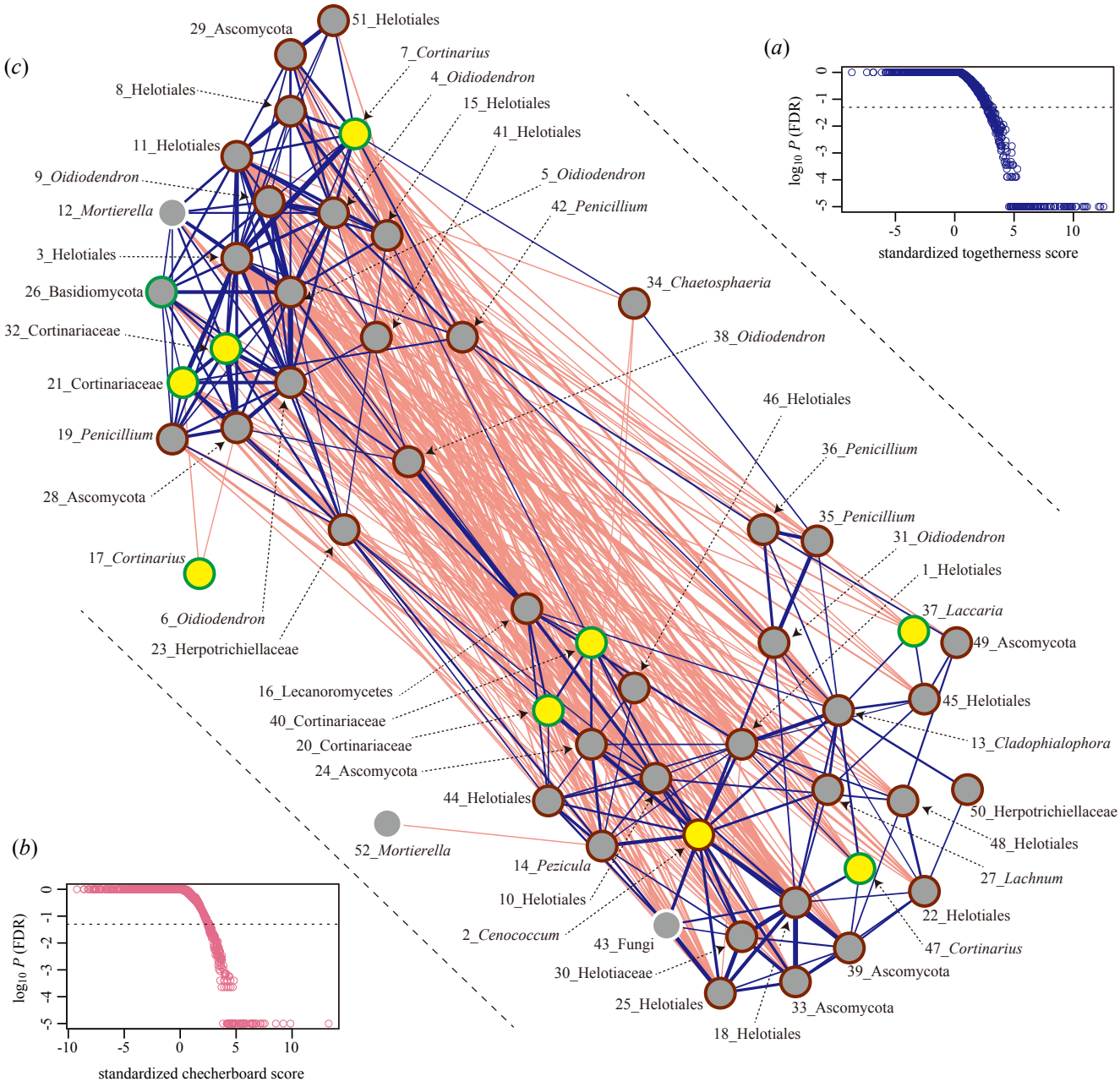
(c)
(a)
(b)
29_Ascomycota
51_Helotiales
7_Cortinarius
4_Oidiodendron
8_Helotiales
15_Helotiales
41_Helotiales
11_Helotiales
5_Oidiodendron
9_Oidiodendron
42_Penicillium
12_Mortierella
3_Helotiales
34_Chaetosphaeria
26_Basidiomycota
32_Cortinariaceae
38_Oidiodendron
21_Cortinariaceae
46_Helotiales
19_Penicillium
36_Penicillium
28_Ascomycota
35_Penicillium
31_Oidiodendron
17_Cortinarius
1_Helotiales
37_Laccaria
6_Oidiodendron
49_Ascomycota
23_Herpotrichiellaceae
16_Lecanoromycetes
45_Helotiales
40_Cortinariaceae
13_Cladophialophora
20_Cortinariaceae
24_Ascomycota
44_Helotiales
50_Herpotrichiellaceae
52_Mortierella
48_Helotiales
14_Pezicula
27_Lachnum
10_Helotiales
22_Helotiales
2_Cenococcum
47_Cortinarius
43_Fungi
39_Ascomycota
30_Helotiaceae
25_Helotiales
33_Ascomycota
18_Helotiales
log10 P (FDR)
standardized togetherness score
standardized checherboard score

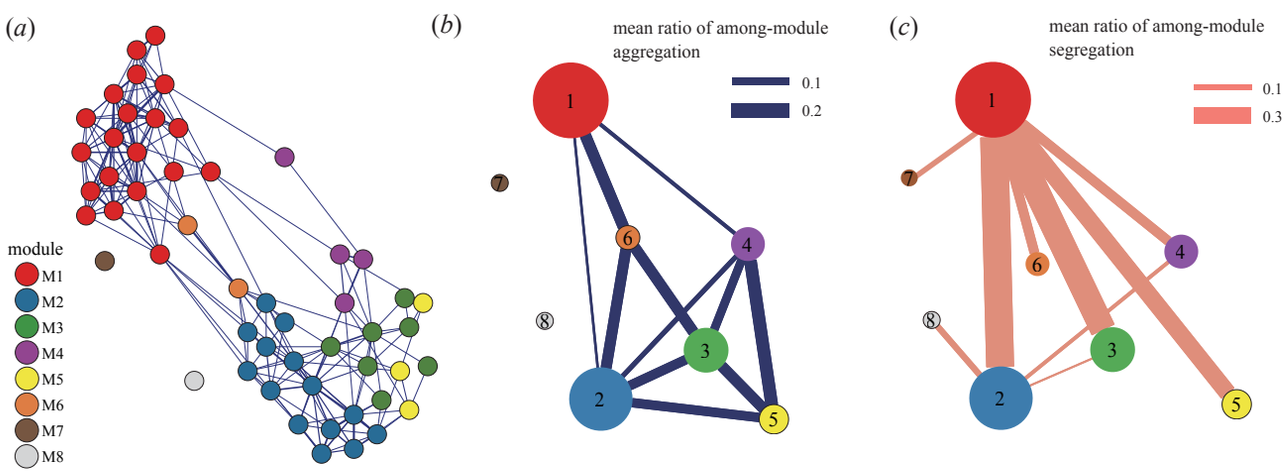
(a)
module
M1
M2
M3
M4
M5
M6
M7
M8
(b)
mean ratio of among-module aggregation
0.1
0.2
1
2
3
4
5
6
7
8
(c)
mean ratio of among-module segregation
0.1
0.3
1
2
3
4
5
6
7
8

Figure 2

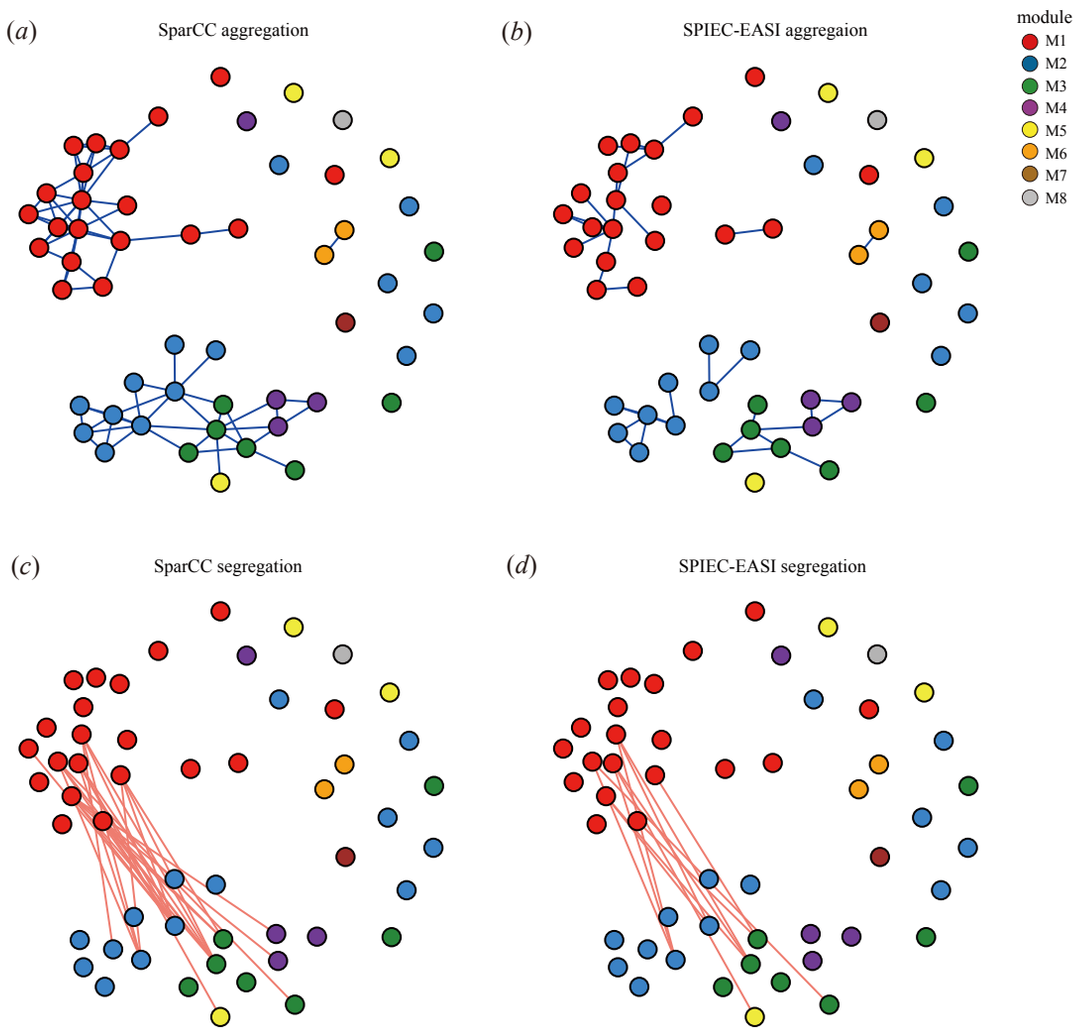
(a)
SparCC aggregation
(b)
SPIEC-EASI aggregaion
module
M1
M2
M3
M4
M5
M6
M7
M8
(c)
SparCC segregation
(d)
SPIEC-EASI segregation

Figure 3

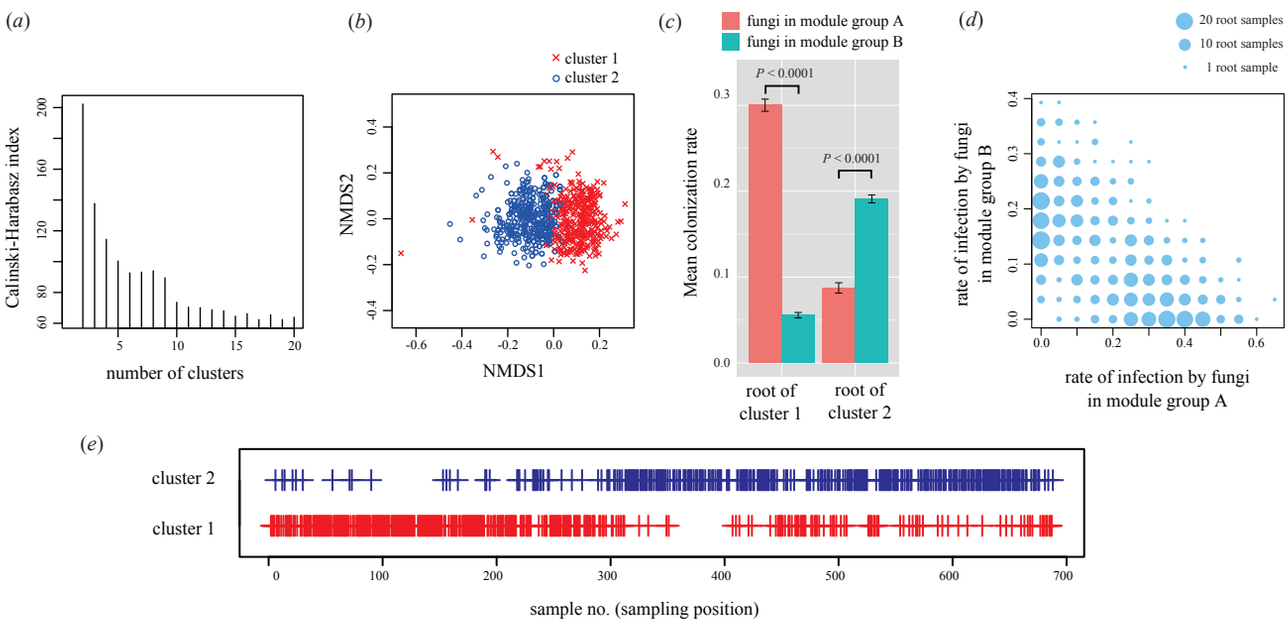
(a)
Calinski-Harabasz index
number of clusters
(b)
cluster 1
cluster 2
NMDS2
NMDS1
(c)
fungi in module group A
fungi in module group B
Mean colonization rate
P < 0.0001
P < 0.0001
root of cluster 1
root of cluster 2
(d)
20 root samples
10 root samples
1 root sample
rate of infection by fungi in module group B
rate of infection by fungi in module group A
(e)
cluster 2
cluster 1
sample no. (sampling position)

Figure 4

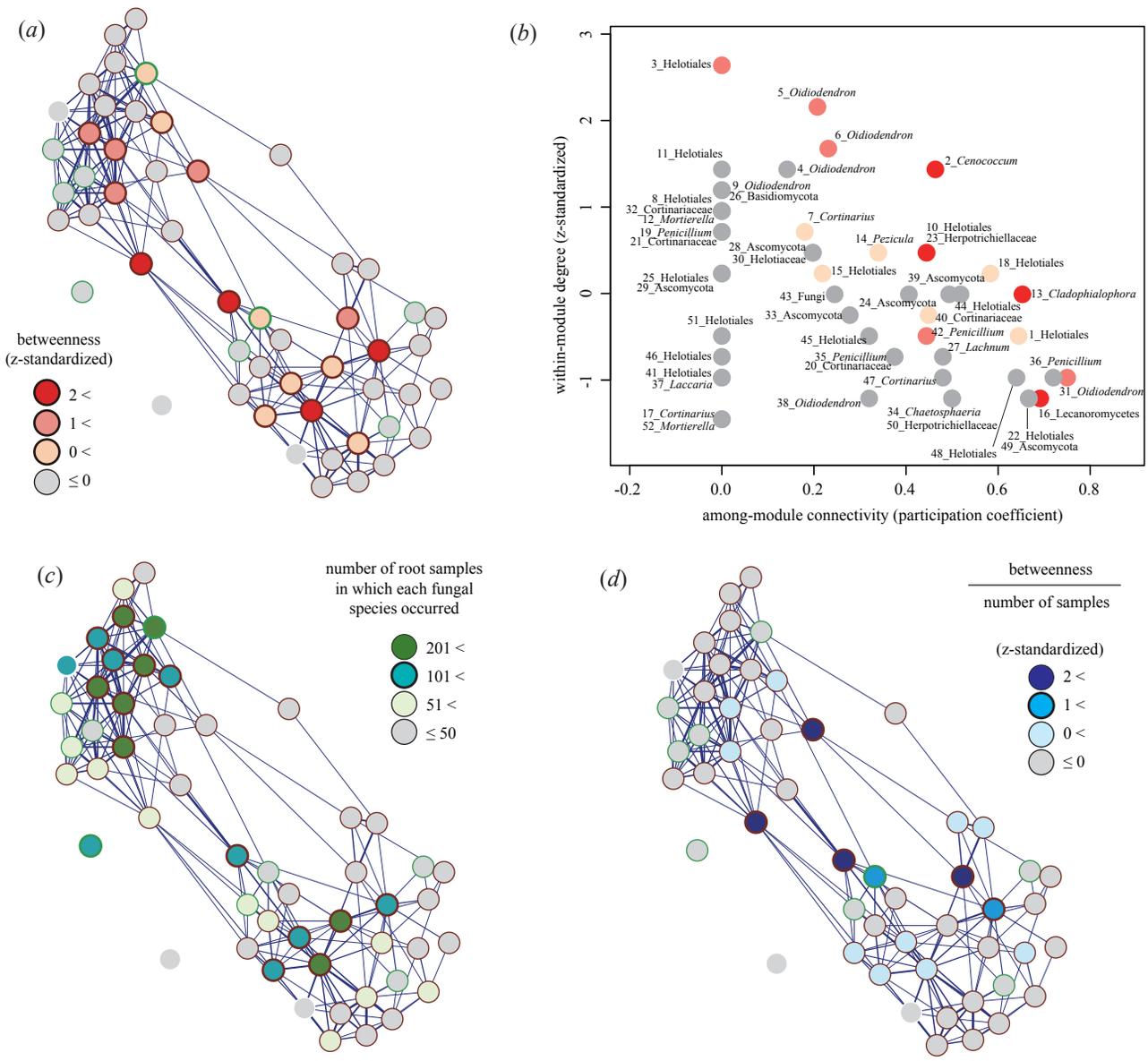
(a)
betweenness
(z-standardized)
2 <
1 <
0 <
≤ 0
(b)
within-module degree (z-standardized)
among-module connectivity (participation coefficient)
3_Helotiales
5_Oidiodendron
6_Oidiodendron
11_Helotiales
4_Oidiodendron
2_Cenococcum
9_Oidiodendron
26_Basidiomycota
8_Helotiales
32_Cortinariaceae
12_Mortierella
7_Cortinarius
19_Penicillium
21_Cortinariaceae
10_Helotiales
23_Herpotrichiellaceae
14_Pezicula
28_Ascomycota
30_Helotiaceae
18_Helotiales
15_Helotiales
25_Helotiales
29_Ascomycota
39_Ascomycota
43_Fungi
24_Ascomycota
13_Cladophialophora
44_Helotiales
33_Ascomycota
40_Cortinariaceae
51_Helotiales
42_Penicillium
1_Helotiales
45_Helotiales
27_Lachnum
46_Helotiales
35_Penicillium
20_Cortinariaceae
36_Penicillium
41_Helotiales
37_Laccaria
47_Cortinarius
31_Oidiodendron
38_Oidiodendron
16_Lecanoromycetes
17_Cortinarius
52_Mortierella
34_Chaetosphaeria
50_Herpotrichiellaceae
22_Helotiales
49_Ascomycota
48_Helotiales
(c)
number of root samples
in which each fungal
species occurred
201 <
101 <
51 <
≤ 50
(d)
betweenness
number of samples
(z-standardized)
2 <
1 <
0 <
≤ 0

Electric Supplementary Material for

Network modules and hubs in plant-root fungal biome

Hirokazu Toju, Satoshi Yamamoto, Akifumi S. Tanabe, Takashi Hayakawa and Hiroshi S. Ishii

Corresponding author:

e-mail: toju.hirokazu.4c@kyoto-u.ac.jp

This PDF file includes:

Method S1

Figures S1-S5

Table S1

Other Electric Supplementary Materials for this manuscript:

Data S1. Data matrix and fungal taxonomic information.

Data S2. ITS1 sequences of the fungi analyzed.

Data S3. Results and data of the aggregation/segregation analysis.

Data S4. Results of togetherness and checkerboard analysis for 5-m interval partial datasets.

Method S1

Clustering analysis of root samples.

The clustering analysis was first performed based on the partial dataset that consisted of the 52 fungal species that occurred 30 or more root samples using the Bray-Curtis β-diversity metric (figure 4*a*, *b*). We then examined the robustness of the results by conducting additional analyses based on the full dataset including 592 fungal species (OTUs) using Bray-Curtis and Chao [1] β-diversity metrics (figure S3). As four root samples (samples nos. 196, 393, 400 and 620) constituted outliers within NMDS plots, they were excluded from the clustering analyses. Due to the exceptional diversity of fungi in the community dataset, summarizing the sample-pairwise distance (β-diversity) matrix in a two-dimensional NMDS plot was basically difficult. That is, even after the "metaMDS" exploration of optimal ordination with the vegan package, stress values remained relatively high (0.225 in figure 4*b*; 0.227 in figure S3*b*; 0.226 in figure S3*e*). Accordingly, several root samples of the cluster 1 were plotted away from the majority of the cluster 1 samples (figure 4; figure S3). As the NMDS is merely a visualization tool, its result does not affect clustering analysis at all. In the clustering and NMDS visualization, the vegan, cluster v2.0.1 and clusterSim v.0.44-2 packages of R were used.

1. Chao, A, Chazdon, RL, Colwell, RK & Shen, TJ. 2005 A new statistical approach for assessing similarity of species composition with incidence and abundance data. *Ecol. Lett.* **8**, 148-159.

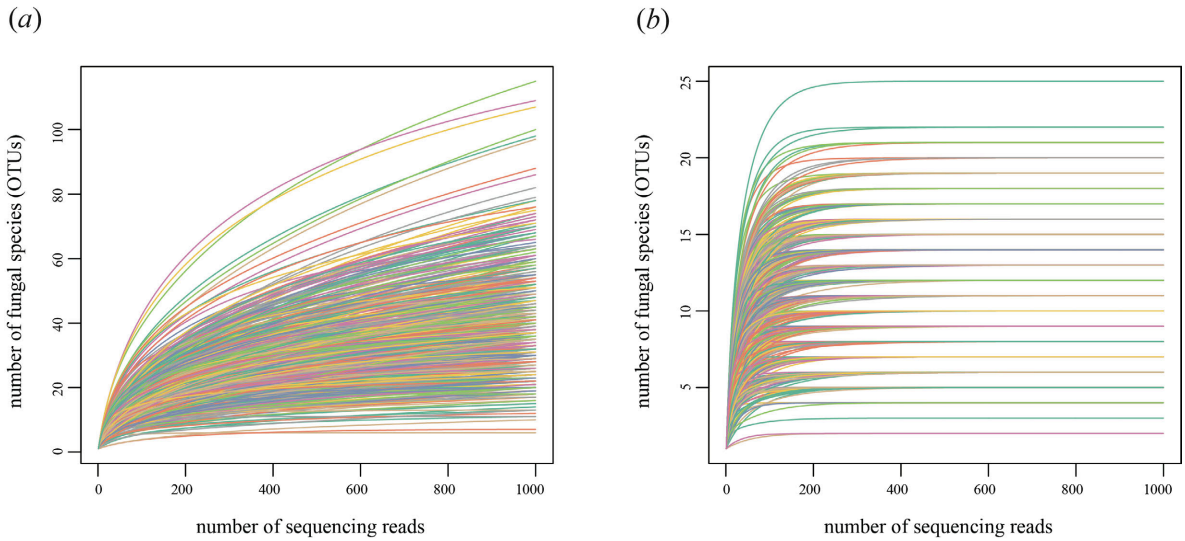

Figure S1. Rarefaction curves of the sequencing reads. (*a*) Dataset before 1%-filtering. Each curve represents relationship between the number of sequencing reads and the number of detected fungal OTUs. (*b*) Dataset after 1%-filtering.

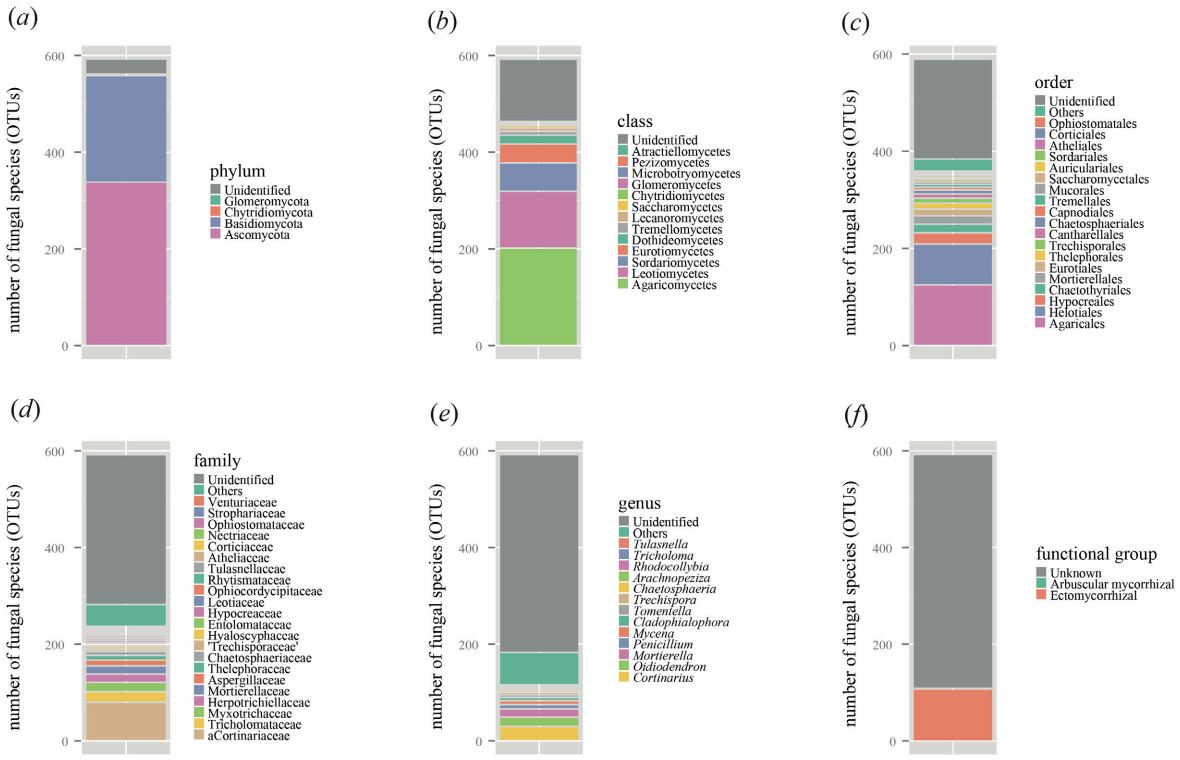

Figure S2. Composition of the 592 fungal species. (*a*) Phylum-level taxonomy. (*b*) Class-level taxonomy. (*c*) Order-level taxonomy. (*d*) Family-level taxonomy. (*e*) Genus-level taxonomy. (*f*) Functional groups.

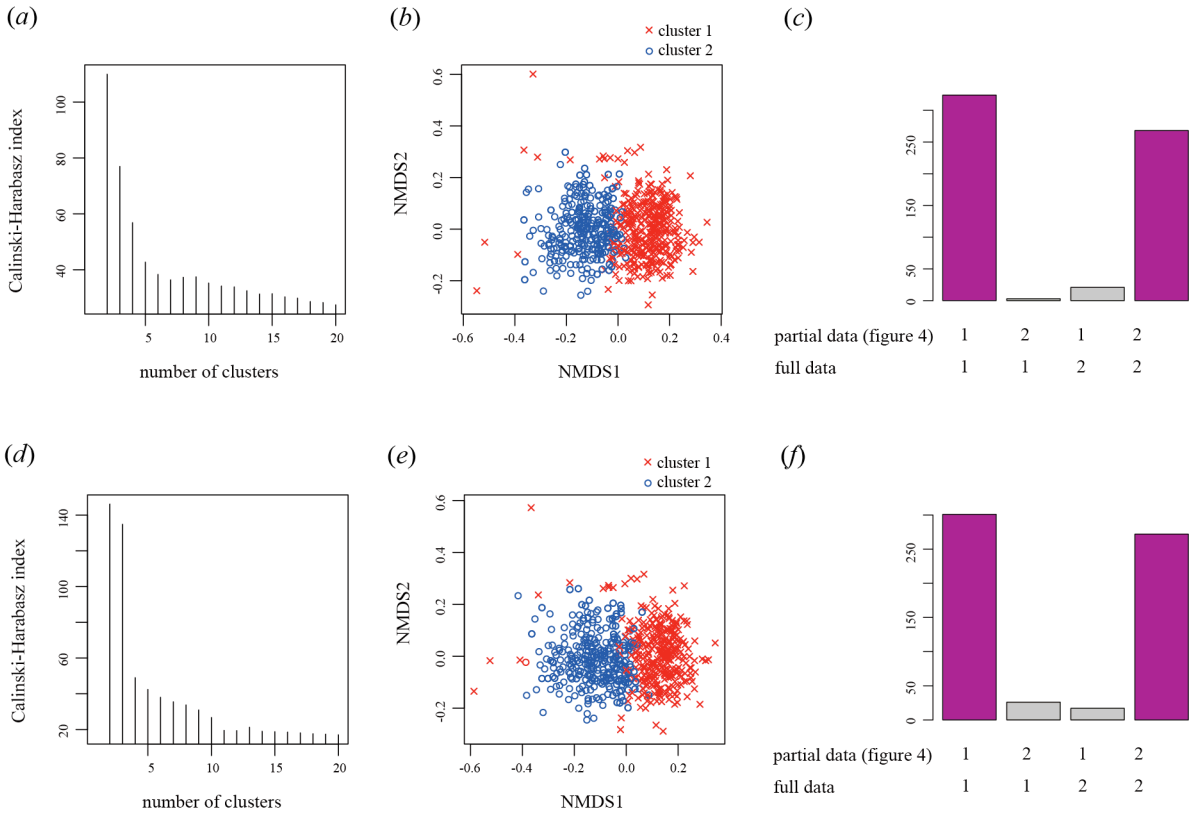

Figure S3. Clustering analysis based on the 592-fungus full dataset. (*a-c*) Analysis with Bray-Curtis *β*-diversity. The number of clusters (i.e., rhizotypes) was estimated to be two based on the analysis with the Calinski-Harabasz index (*a*) A NMDS plot showing the fungal community composition of the root samples is presented (*b*). The clustering results based on the full data set was compared with those of figure 4, in which only the fungal species that occurred 30 or more root samples were analyzed (*c*). (*d-f*) Analysis with Chao *β*-diversity.

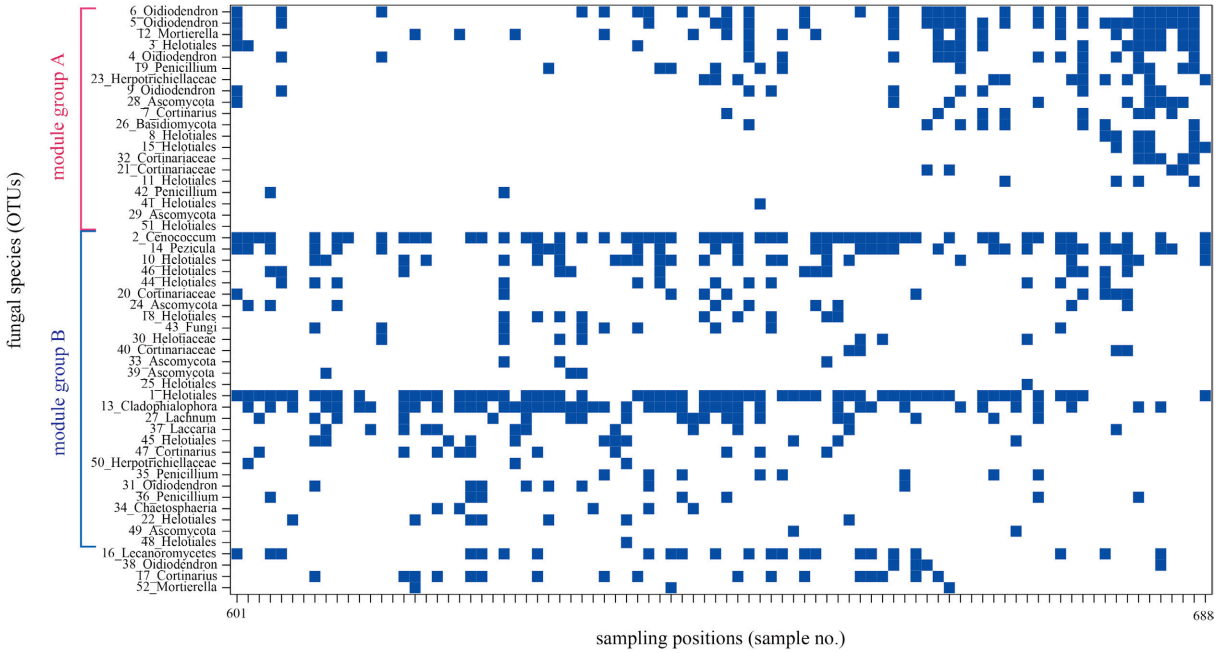

Figure S4. Spatial patterns in the occurrence of each fungal species. The presence/absence of the fungal species (OTUs) appeared in the symbiont–symbiont co-occurrence network is shown for each sampling position. For simplicity, the information of the sampling positions 601 through 688 is presented.

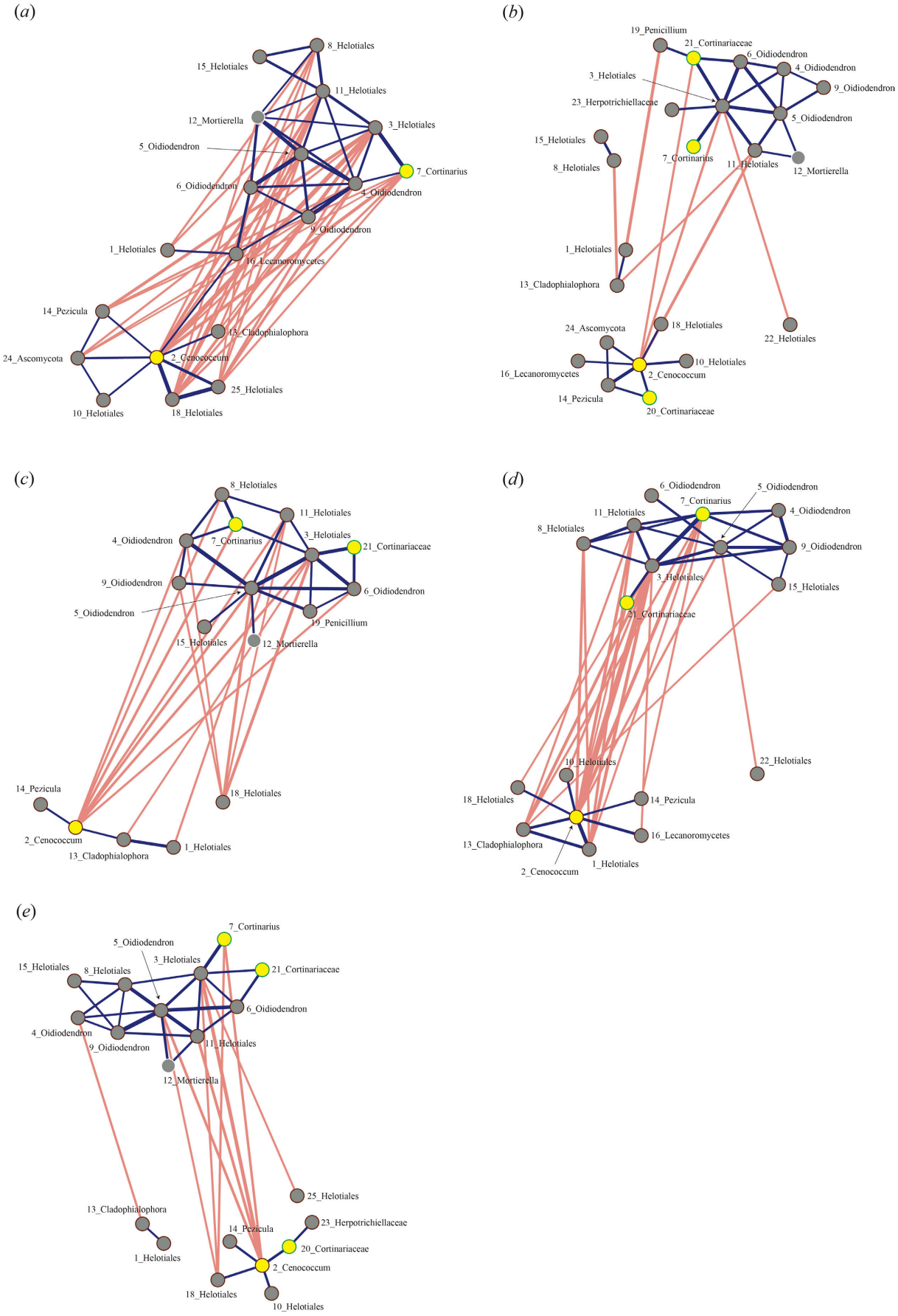
(a)
8_Helotiales
15_Helotiales
11_Helotiales
12_Mortierella
3_Helotiales
5_Oidiodendron
7_Cortinarius
6_Oidiodendron
4_Oidiodendron
9_Oidiodendron
1_Helotiales
16_Lecanoromycetes
14_Pezicula
13_Cladophialophora
24_Ascomycota
2_Cenococcum
25_Helotiales
10_Helotiales
18_Helotiales
(b)
19_Penicillium
21_Cortinariaceae
6_Oidiodendron
4_Oidiodendron
3_Helotiales
9_Oidiodendron
23_Herpotrichiellaceae
5_Oidiodendron
15_Helotiales
7_Cortinarius
11_Helotiales
12_Mortierella
8_Helotiales
1_Helotiales
13_Cladophialophora
24_Ascomycota
18_Helotiales
22_Helotiales
10_Helotiales
16_Lecanoromycetes
2_Cenococcum
14_Pezicula
20_Cortinariaceae
(c)
8_Helotiales
11_Helotiales
4_Oidiodendron
7_Cortinarius
3_Helotiales
21_Cortinariaceae
9_Oidiodendron
6_Oidiodendron
5_Oidiodendron
19_Penicillium
15_Helotiales
12_Mortierella
14_Pezicula
18_Helotiales
2_Cenococcum
1_Helotiales
13_Cladophialophora
(d)
6_Oidiodendron
5_Oidiodendron
7_Cortinarius
11_Helotiales
4_Oidiodendron
8_Helotiales
9_Oidiodendron
3_Helotiales
15_Helotiales
21_Cortinariaceae
22_Helotiales
10_Helotiales
18_Helotiales
14_Pezicula
16_Lecanoromycetes
13_Cladophialophora
1_Helotiales
2_Cenococcum
(e)
7_Cortinarius
5_Oidiodendron
3_Helotiales
15_Helotiales
8_Helotiales
21_Cortinariaceae
6_Oidiodendron
4_Oidiodendron
9_Oidiodendron
11_Helotiales
12_Mortierella
25_Helotiales
13_Cladophialophora
23_Herpotrichiellaceae
14_Pezicula
20_Cortinariaceae
1_Helotiales
2_Cenococcum
18_Helotiales
10_Helotiales

Figure S5. Symbiont–symbiont networks estimated based on the 5-m interval partial datasets. For each of the 5-m interval partial datasets, the aggregation and segregation of pairs of fungal species were analyzed based on the togetherness and checkerboard scores, respectively. Fungal species are linked by lines indicating statistically significant (FDR < 0.05) aggregation (blue) and segregation (red). The thickness of links is proportional to standardized togetherness or checkerboard scores. The circles representing fungal species (yellow, ectomycorrhizal fungi; gray, fungi with unknown functions) are placed based on the aggregation patterns with the ForceAtlas2 algorithm. The outer parts of the circles represent fungal taxonomy (brown, Ascomycota; green; Basidiomycota; white, unidentified). (*a*) Partial dataset 1. (*b*) Partial dataset 2. (*c*) Partial dataset 3. (*d*) Partial dataset 4. (*e*) Partial dataset 5.

Table S1. Fungi that appeared in 30 or more samples. Fungal OTUs belonging to the module group A (module 1) and module group B (modules 2–5) are highlighted in red and blue, respectively. The two module groups included both ectomycorrhizal and possibly endophytic fungal lineages. The information of the lowest taxonomic rank assigned by the UCLUST algorithm with UNITE ver.7 dynamic database is also shown.

OTU	Module	*N*.sample	Phylum	Class	Order	Family	Genus	Functional.group	UNITE
F3	A (1)	245	Ascomycota	Leotiomycetes	Helotiales			Unknown	Dermateaceae
F4	A (1)	237	Ascomycota	Leotiomycetes		Myxotrichaceae	*Oidiodendron*	Unknown	*Oidiodendron*
F5	A (1)	235	Ascomycota	Leotiomycetes		Myxotrichaceae	*Oidiodendron*	Unknown	*Oidiodendron*
F6	A (1)	222	Ascomycota	Leotiomycetes		Myxotrichaceae	*Oidiodendron*	Unknown	*Oidiodendron*
F7	A (1)	210	Basidiomycota	Agaricomycetes	Agaricales	Cortinariaceae	*Cortinarius*	Ectomycorrhizal	*Cortinarius*
F8	A (1)	207	Ascomycota	Leotiomycetes	Helotiales			Unknown	Helotiales
F9	A (1)	161	Ascomycota	Leotiomycetes		Myxotrichaceae	*Oidiodendron*	Unknown	*Oidiodendron*
F11	A (1)	144	Ascomycota	Leotiomycetes	Helotiales			Unknown	Unassigned
F12	A (1)	134			Mortierellales	Mortierellaceae	*Mortierella*	Unknown	*Mortierella*
F15	A (1)	114	Ascomycota	Leotiomycetes	Helotiales			Unknown	Unassigned
F19	A (1)	93	Ascomycota	Eurotiomycetes	Eurotiales	Aspergillaceae	*Penicillium*	Unknown	*Penicillium*
F21	A (1)	86	Basidiomycota	Agaricomycetes	Agaricales	Cortinariaceae		Ectomycorrhizal	Cortinariaceae
F23	A (1)	70	Ascomycota	Eurotiomycetes	Chaetothyriales	Herpotrichiellaceae		Unknown	Herpotrichiellaceae
F26	A (1)	54	Basidiomycota					Unknown	Sporidiobolales
F28	A (1)	52	Ascomycota					Unknown	Herpotrichiellaceae
F29	A (1)	51	Ascomycota					Unknown	Unassigned
F32	A (1)	47	Basidiomycota	Agaricomycetes	Agaricales	Cortinariaceae		Ectomycorrhizal	*Cortinarius*
F41	A (1)	38	Ascomycota	Leotiomycetes	Helotiales			Unknown	Helotiales
F42	A (1)	38	Ascomycota	Eurotiomycetes	Eurotiales	Aspergillaceae	*Penicillium*	Unknown	*Penicillium*
F51	A (1)	30	Ascomycota	Leotiomycetes	Helotiales			Unknown	Leotiomycetes
F1	B (3)	275	Ascomycota	Leotiomycetes	Helotiales			Unknown	Helotiales
F2	B (2)	270	Ascomycota	Dothideomycetes		Gloniaceae	*Cenococcum*	Ectomycorrhizal	*Cenococcum*
F10	B (2)	159	Ascomycota	Leotiomycetes	Helotiales			Unknown	Helotiales
F13	B (3)	117	Ascomycota	Eurotiomycetes	Chaetothyriales	Herpotrichiellaceae	*Cladophialophora*	Unknown	*Cladophialophora*
F14	B (2)	114	Ascomycota	Leotiomycetes	Helotiales	Dermateaceae	*Pezicula*	Unknown	Dermateaceae
F18	B (2)	98	Ascomycota	Leotiomycetes	Helotiales			Unknown	Helotiales
F20	B (2)	87	Basidiomycota	Agaricomycetes	Agaricales	Cortinariaceae		Ectomycorrhizal	*Cortinarius*
F22	B (5)	77	Ascomycota	Leotiomycetes	Helotiales			Unknown	Helotiales
F24	B (2)	64	Ascomycota					Unknown	Unassigned
F25	B (2)	63	Ascomycota	Leotiomycetes	Helotiales			Unknown	Helotiales
F27	B (3)	52	Ascomycota	Leotiomycetes	Helotiales	Hyaloscyphaceae	*Lachnum*	Unknown	*Lachnum*

F30	B (2)	48	Ascomycota	Leotiomycetes	Helotiales	Helotiaceae		Unknown	Leotiomycetes
F33	B (2)	47	Ascomycota					Unknown	Vibrisseaceae
F31	B (4)	47	Ascomycota	Leotiomycetes		Myxotrichaceae	*Oidiodendron*	Unknown	*Oidiodendron*
F34	B (4)	46	Ascomycota	Sordariomycetes	Chaetosphaeriales	Chaetosphaeriaceae	*Chaetosphaeria*	Unknown	*Chaetosphaeria*
F35	B (4)	46	Ascomycota	Eurotiomycetes	Eurotiales	Aspergillaceae	*Penicillium*	Unknown	*Penicillium*
F36	B (4)	46	Ascomycota	Eurotiomycetes	Eurotiales	Aspergillaceae	*Penicillium*	Unknown	*Penicillium*
F37	B (3)	44	Basidiomycota	Agaricomycetes	Agaricales	Tricholomataceae	*Laccaria*	Ectomycorrhizal	Agaricales
F39	B (2)	42	Ascomycota					Unknown	Unassigned
F40	B (2)	41	Basidiomycota	Agaricomycetes	Agaricales	Cortinariaceae		Ectomycorrhizal	*Cortinarius*
F43	B (2)	38						Unknown	*Oidiodendron*
F44	B (2)	37	Ascomycota	Leotiomycetes	Helotiales			Unknown	Ascomycota
F45	B (3)	35	Ascomycota	Leotiomycetes	Helotiales			Unknown	Leotiomycetes
F46	B (2)	34	Ascomycota	Leotiomycetes	Helotiales			Unknown	Helotiales
F47	B (3)	33	Basidiomycota	Agaricomycetes	Agaricales	Cortinariaceae	*Cortinarius*	Ectomycorrhizal	*Cortinarius*
F48	B (5)	33	Ascomycota	Leotiomycetes	Helotiales			Unknown	Unassigned
F49	B (5)	32	Ascomycota					Unknown	Helotiales
F50	B (3)	31	Ascomycota	Eurotiomycetes	Chaetothyriales	Herpotrichiellaceae		Unknown	Fungi
F16	6	110	Ascomycota	Lecanoromycetes				Unknown	Unassigned
F17	7	100	Basidiomycota	Agaricomycetes	Agaricales	Cortinariaceae	*Cortinarius*	Ectomycorrhizal	*Cortinarius*
F38	6	43	Ascomycota	Leotiomycetes		Myxotrichaceae	*Oidiodendron*	Unknown	*Oidiodendron*
F52	8	30			Mortierellales	Mortierellaceae	*Mortierella*	Unknown	*Mortierella*

97

98